J Elast (2011) 102: 99–116
DOI 10.1007/s10659-010-9264-7

An 8-chain Model for Rubber-like Materials Accounting for Non-affine Chain Deformations and Topological Constraints

Martin Kroon

Received: 18 February 2010 / Published online: 11 June 2010

Abstract Several industrial applications involve rubber and rubber-like materials, and it is important to be able to predict the constitutive response of these materials. In the present paper, a new constitutive model for rubber-like solids is proposed. The model is based on the 8-chain concept introduced by Arruda and Boyce (J. Mech. Phys. Solids 41, 389–412, 1993) to which two new components are added. Real polymer networks do not deform affinely, and in the proposed model this is accounted for by the inclusion of an elastic spring, acting in series with the representative polymer chain. Furthermore, real polymer chains are not completely free to move, which is modelled by imposing a topological constraint on the transverse motions of the representative polymer chain. The model contains five model parameters and these need to be determined on the basis of experimental data. Three experimental studies from the literature were used to assess the proposed model. The model was able to reproduce experimental data performed under conditions of uniaxial tension, generalised plane deformation, and biaxial tension with an excellent accuracy. The strong predictive abilities together with the numerically efficient structure of the model make it suitable for implementation in a finite element context.

Keywords Rubber · Elastomer · Hyperelastic · Strain energy · Non-affine · Tube model

Mathematics Subject Classification (2000) 74B20 · 82D60

1 Introduction

Rubber and rubber-like materials are used in a wide range of industrial applications, such as tires, seals, conveyor belts, base isolations of buildings, bridge bearings, etc. To attain appropriate designs of rubber components under different types of mechanical loading, it is important to have access to accurate constitutive models for rubber that are applicable under multiaxial loading conditions.

M. Kroon (✉)
Royal Institute of Technology (KTH), Osquars backe 1, 100 44 Stockholm, Sweden
e-mail: martin@hallf.kth.se

Rubber-like materials are extremely deformable, and upon unloading, the initial configuration is almost completely recovered. Thus, these materials are often assumed to be fully elastic. It is therefore convenient to formulate the constitutive behaviour in terms of a strain energy function. The elasticity of rubbers is governed by the entropy of the long polymer chains that constitute the rubber. By use of statistical mechanics, the elastic behaviour of single chains can be analysed and predicted [1–6]. Based on these analyses, constitutive models have been proposed in terms of a strain energy. The Gaussian treatment leads to the so-called neo-Hookean model. If the finite extensibility of the polymer chains is taken into account, the strain energy of the polymer chains can be approximated by use of Langevin statistics. Several representative polymer chains may then be combined into a model to predict the 3D behaviour of rubber. In the so-called *3-chain model* [5, 7], it is assumed that the network of polymer chains can be represented by three chains, oriented in the three principal directions of deformation. The *4-chain model* [8, 9] instead models the polymer network by use of four representative polymer chains, which are connected to the corners of a tetrahedron and a central junction. In the *8-chain model* by Arruda and Boyce [10], eight chains are used to represent the polymer network. The representative chains are then attached to the corners of a cube and a central junction. In the model by Elias-Zuniga and Beatty [11], the *3-chain model* and the *8-chain model* are combined. Finally, if the representative chains are taken to be distributed over all possible orientations, the *full network model* is attained [12–16].

Most of the previous models of rubber elasticity were not able to fully account for the stress-strain relations under multiaxial loading conditions. Models aiming at taking topological constraint effects in the polymer networks into account were therefore developed. In the *constrained junction* theories [17–21], the topological constraints around the junctions in a polymer chain are modelled. The *constrained segment* theories (*tube* models) constitute an alternative approach [22–26], where interaction effects along the chain contour are instead modelled.

In addition to the statistical mechanics-based models mentioned above, there are also a number of phenomenological models for rubber-like materials available in the literature, see for example Horgan and Saccomandi [27] for a review. In the models by Mooney-Rivlin [28, 29], Gent [30, 31], Yeoh [32], and Beda [33], the strain energy of the rubber material is expressed by use of the invariants of the deformation state. In the models by Valanis and Landel [34] and Ogden [35], the strain energy is instead expressed as a polynomial of the principal stretches. The Mooney-Rivlin model may, however, be related to statistical mechanics [36].

In the present paper, a new constitutive model for rubber-like materials is proposed. The model is based on the 8-chain approach proposed by Arruda and Boyce [10], but is expanded to account for non-affine polymer chain deformations and for topological constraints according to the tube theory. The model contains five parameters that need to be determined on the basis of experiments. The influence of the different parameters is illustrated, and the model is compared to experimental results from the literature.

2 Model Description

2.1 Strain Energy of Representative Polymer Chain

We start by considering a single representative polymer chain, see Fig. 1. The chain is taken to consist of n segments of equal length l. The distance between the end points of the chain

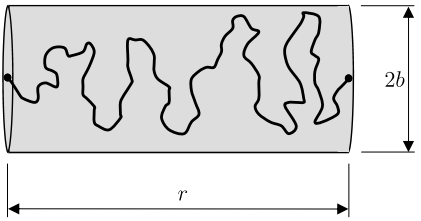

Fig. 1 Geometry of the representative polymer chain. The distance between the end points is denoted r and the radius of the constraint cylinder is denoted b

is r, and the maximum length of the chain is $r_{\max} = nl$. According to random walk theory, the root-mean-square value of r for an unstrained chain is $r_0 = \sqrt{n}l$. The stretch of the chain is then defined as

$$\lambda_c = \frac{r}{r_0}. \tag{1}$$

We assume that, due to the interaction with surrounding polymer chains, the geometry of the representative polymer chain is confined to a tube with a radius b, see Fig. 1. In the undeformed configuration, this radius is taken to be b_0. Following Doi and Edwards [37] and Miehe et al. [16], we introduce the variable ν, defined as

$$\nu = (b_0/b)^2. \tag{2}$$

The infinitesimal probability $\mathrm{d}P$ that the conformation of the chain falls in the geometry range $[\lambda_c, \lambda_c + \mathrm{d}\lambda_c]$ and $[\nu, \nu + \mathrm{d}\nu]$ can be expressed as

$$\mathrm{d}P(\lambda_c, \nu) = p(\lambda_c, \nu)\mathrm{d}\lambda_c\mathrm{d}\nu. \tag{3}$$

The probability density $p(\lambda_c, \nu)$ is assumed to be of the form

$$p(\lambda_c, \nu) = p_\lambda(\lambda_c)\, p_\nu(\nu), \tag{4}$$

where $p_\lambda(\lambda_c)$ and $p_\nu(\nu)$ are two probability densities that independently describe the stretching of the chain and the tube constraint, respectively. To account for the finite extensibility of the chain, inverse Langevin statistics is employed. Thus, the probability density $p_\lambda(\lambda_c)$ is expressed as

$$p_\lambda(\lambda_c) = \gamma_\lambda \exp\left\{-n\left(\frac{\lambda_c}{\sqrt{n}}\beta + \ln\frac{\beta}{\sinh\beta}\right)\right\}, \tag{5}$$

where γ_λ is a normalisation constant and β is defined by the Langevin function

$$\coth\beta - \frac{1}{\beta} = \frac{\lambda_c}{\sqrt{n}}. \tag{6}$$

The probability of the straight tube constraint is given the form

$$p_\nu(\nu) = \gamma_\nu \exp\left\{-\alpha\left(\frac{r_0}{b_0}\right)^2 \nu\right\} \tag{7}$$

[37], where γ_ν is a normalisation constant and α is a material constant.

The entropy s of this representative chain is now given by Boltzmann's equation

$$s = k_{\mathrm{B}} \cdot \ln p, \tag{8}$$

where k_{B} is Boltzmann's constant. For purely entropic elasticity, the change in strain energy $\Delta\Psi_{\mathrm{c}}$ during deformation of the chain is given by

$$\Delta\Psi_{\mathrm{c}} = -T\,\Delta s, \tag{9}$$

where Δs is the associated change in entropy and T is the absolute temperature. The strain energy Ψ_{c} of this chain may then be expressed as

$$\Psi_{\mathrm{c}} = k_{\mathrm{B}} T n \left\{ \frac{\lambda_{\mathrm{c}}}{\sqrt{n}}\beta + \ln\frac{\beta}{\sinh\beta} + \alpha\left(\frac{l}{b_0}\right)^2 \nu \right\} + \Psi_{\mathrm{c}0}, \tag{10}$$

where $\Psi_{\mathrm{c}0}$ is a constant.

We now introduce the stretch λ_{m}, which is the macroscopic stretch imposed on the rubber material in the direction of the polymer chain. If the polymer chain deforms affinely, the relation $\lambda_{\mathrm{c}} = \lambda_{\mathrm{m}}$ will hold. However, in a real polymer network, this is not the case. Instead, when a polymer chain is stretched so that it approaches its maximum extensibility, it will deform less than the macroscopic stretch and will thus not deform affinely. As a consequence, other chains in the surrounding polymer network will need to deform more than what is predicted by the macroscopic stretch. In order to account for this effect, the macroscopic stretch λ_{m} is decomposed according to

$$\lambda_{\mathrm{m}} = \lambda_{\mathrm{c}}\lambda_{\mathrm{nc}}, \tag{11}$$

where λ_{nc} is a stretch associated with the additional compliance from the surrounding polymer network, see Fig. 2. Thus, $\lambda_{\mathrm{nc}} = 1$ corresponds to a fully affine deformation of the representative polymer chain. But in general, the surrounding polymer network will contribute with some serial compliance, associated with a stretch $\lambda_{\mathrm{nc}} \neq 1$, and the representative polymer chain will then deform non-affinely.

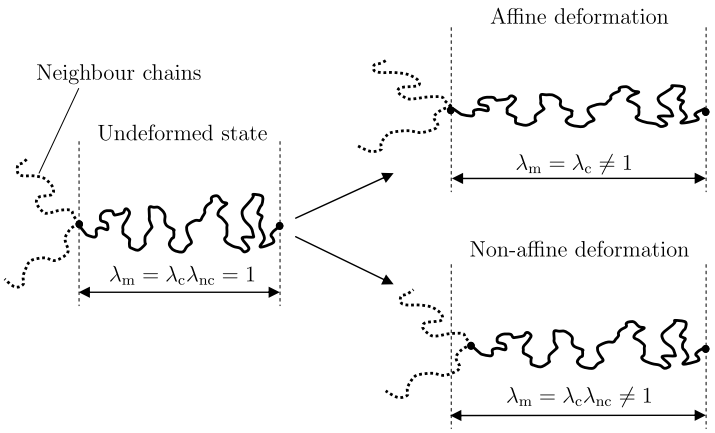

Fig. 2 Affine and non-affine deformation of the representative polymer chain

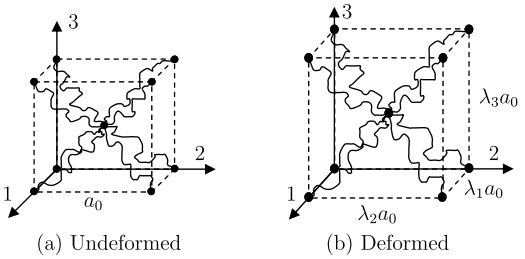

(a) Undeformed (b) Deformed

Fig. 3 Arrangement of representative chains in 8-chain model. Directions 1, 2, and 3 denote the principal directions of deformation, and a_0 is the side length of the undeformed cube containing the 8 chains

2.2 Strain Energy of Polymer Network

We now consider the strain energy of a polymer network constituting the rubber material. The position vectors in the reference and deformed states of the material are denoted by $\mathbf{X}$ and $\mathbf{x}$, respectively. The deformation gradient is computed as $\mathbf{F} = \partial\mathbf{x}/\partial\mathbf{X}$, and the Jacobian is $J = \det\mathbf{F}$. The right Cauchy-Green deformation tensor is computed as $\mathbf{C} = \mathbf{F}^{\mathrm{T}}\mathbf{F}$, and the principal stretches λ_1, λ_2, and λ_3 are related to the deformation invariants I_1, I_2, I_3 of $\mathbf{C}$ according to

$$I_1 = \lambda_1^2 + \lambda_2^2 + \lambda_3^2, \qquad I_2 = \lambda_1^2\lambda_2^2 + \lambda_1^2\lambda_3^2 + \lambda_2^2\lambda_3^2, \qquad I_3 = \lambda_1^2\lambda_2^2\lambda_3^2. \tag{12}$$

Incompressibility is assumed, implying $I_3 = J^2 = 1$.

In the 8-chain model by Arruda and Boyce [10], the polymer network constituting the rubber material is represented by eight identical polymer chains, which are connected to the corners of a cube and a central junction, see Fig. 3. During deformation of the material, the sides of the cube remain parallel to the principal directions of deformation. For the eight representative chains in the 8-chain model, the stretch λ_{m} is related to the multiaxial deformation state according to

$$\lambda_{\mathrm{m}} = \left(\frac{1}{3}\left(\lambda_1^2 + \lambda_2^2 + \lambda_3^2\right)\right)^{1/2} = \left(\frac{I_1}{3}\right)^{1/2}. \tag{13}$$

Nanson's formula is employed to compute ν (cf. [37] and [16]). This formula relates vector elements of infinitesimally small areas $\mathrm{d}\mathbf{S}$ and $\mathrm{d}\mathbf{s}$ in the reference and deformed states, respectively, according to $\mathrm{d}\mathbf{s} = J^{-1}\mathbf{F}^{-\mathrm{T}}\mathrm{d}\mathbf{S}$. If the principal directions of the deformation in the reference configuration are given by the unit vectors $\mathbf{N}_1$, $\mathbf{N}_2$, and $\mathbf{N}_3$, the 8 chains are oriented in the directions $\mathbf{M} = (\pm\mathbf{N}_1 \pm \mathbf{N}_2 \pm \mathbf{N}_3)/\sqrt{3}$. For the eight representative chains, ν is related to the macroscopic deformation as

$$\begin{aligned}\nu &= \left|J^{-1}\mathbf{F}^{-\mathrm{T}}\mathbf{M}\right| = \left(J^{-2}\mathbf{M}\mathbf{C}^{-1}\mathbf{M}\right)^{1/2} \\ &= \left(\frac{1}{3J^2}\left(\frac{1}{\lambda_1^2} + \frac{1}{\lambda_2^2} + \frac{1}{\lambda_3^2}\right)\right)^{1/2} = \frac{1}{I_3}\left(\frac{I_2}{3}\right)^{1/2} = \left(\frac{I_2}{3}\right)^{1/2},\end{aligned} \tag{14}$$

where the incompressibility condition $I_3 = 1$ has been utilised.

It has been noted, that strain energy functions only including a dependence on I_1 are unable to accurately capture the constitutive behaviour of rubber at low to moderate strains [38–40]. In the present model, the constraint parameter ν introduces an additional dependence on the invariant I_2 in a natural way. As mentioned above, a dependence on I_2 may also be motivated on the basis of statistical mechanics [36].

Based on the expression for the strain energy of a single representative chain derived in the previous subsection, the following strain energy Ψ is now proposed for the rubber material:

$$\Psi = c_c n \left(\frac{\lambda_c}{\sqrt{n}} \beta + \ln \frac{\beta}{\sinh \beta} \right) + c_{nc} \left(\lambda_{nc}^2 - 1 \right)^{\alpha} + c_{con} n \nu - p(J-1). \tag{15}$$

In the expression for Ψ above, c_c, c_{nc}, α, and c_{con} are material constants, λ_c and λ_{nc} relate through (11), β is defined through (6), λ_m is given by (13), and ν is given by (14). The first term in (15) represents the strain energy of the representative polymer chains, the second term penalises non-affine deformations, and the third term accounts for the tube constraint on the polymer chains. To account for incompressibility, the strain energy function is also supplied with a fourth term that penalises volumetric changes, where p is a Lagrange multiplier. Thus, in total there are five material constants in the proposed model: n, c_c, c_{nc}, α, and c_{con}.

In principle, the strain energy in (15) depends on three independent deformation entities, namely λ_m, λ_{nc}, and ν. For a given macroscopic deformation state $\mathbf{F}$, the entities λ_m and ν are directly defined by (13) and (14), but λ_{nc} remains to be determined. Thus, for a given deformation state $\mathbf{F}$ (which sets λ_m and ν), λ_{nc} is taken to adjust so that the strain energy Ψ is minimised. Thus, the additional condition

$$\left. \frac{\partial \Psi(\lambda_m, \lambda_{nc}, \nu)}{\partial \lambda_{nc}} \right|_{\lambda_m, \nu} = -c_c \sqrt{n} \beta \frac{\lambda_m}{\lambda_{nc}^2} + 2 c_{nc} \alpha \lambda_{nc} \left(\lambda_{nc}^2 - 1 \right)^{\alpha - 1} = 0 \tag{16}$$

is applied. Note that β also depends on λ_{nc} through λ_c. Equation (16) is a non-linear relation that needs to be solved for λ_{nc}.

2.3 Computation of Stress Tensors

The second Piola-Kirchhoff stress tensor $\mathbf{S}$ is obtained as

$$\begin{aligned} \mathbf{S} &= 2 \frac{\partial \Psi}{\partial \mathbf{C}} \\ &= 2 c_c \sqrt{n} \beta \frac{\partial \lambda_c}{\partial \mathbf{C}} + 4 c_{nc} \alpha \left(\lambda_{nc}^2 - 1 \right)^{\alpha - 1} \frac{\partial \lambda_{nc}}{\partial \mathbf{C}} + 2 c_{con} n \frac{\partial \nu}{\partial \mathbf{C}} - p \mathbf{C}^{-1}. \end{aligned} \tag{17}$$

We introduce the relations $\partial I_1 / \partial \mathbf{C} = \mathbf{I}$, $\partial I_2 / \partial \mathbf{C} = I_1 \mathbf{I} - \mathbf{C}$, and $\partial I_3 / \partial \mathbf{C} = I_3 \mathbf{C}^{-1}$, where $\mathbf{I}$ is the identity tensor. The partial derivatives in (17) may then be expressed as

$$\frac{\partial \lambda_c}{\partial \mathbf{C}} = \left(\frac{\partial \lambda_c}{\partial \lambda_m} + \frac{\partial \lambda_c}{\partial \lambda_{nc}} \frac{\mathrm{d}\lambda_{nc}}{\mathrm{d}\lambda_m} \right) \frac{\partial \lambda_m}{\partial \mathbf{C}} = \left(\frac{1}{\lambda_{nc}} - \frac{\lambda_m}{\lambda_{nc}^2} \frac{\mathrm{d}\lambda_{nc}}{\mathrm{d}\lambda_m} \right) \frac{\mathbf{I}}{6\lambda_m}, \tag{18}$$

$$\frac{\partial \lambda_{nc}}{\partial \mathbf{C}} = \frac{\mathrm{d}\lambda_{nc}}{\mathrm{d}\lambda_m} \frac{\partial \lambda_m}{\partial \mathbf{C}} = \frac{\mathrm{d}\lambda_{nc}}{\mathrm{d}\lambda_m} \frac{\mathbf{I}}{6\lambda_m}, \tag{19}$$

$$\frac{\partial \nu}{\partial \mathbf{C}} = \frac{\nu}{2 I_2 I_3} \left(I_3 \frac{\partial I_2}{\partial \mathbf{C}} - 2 I_2 \frac{\partial I_3}{\partial \mathbf{C}} \right) = \frac{\nu}{2 I_2} \left(I_1 \mathbf{I} - \mathbf{C} - 2 I_2 \mathbf{C}^{-1} \right). \tag{20}$$

Differentiation of (16) yields the relation

$$\left(\eta_1 \frac{\mathrm{d}\beta}{\mathrm{d}\lambda_c} + \beta \right) \mathrm{d}\lambda_m + \left(\eta_2 \frac{\mathrm{d}\beta}{\mathrm{d}\lambda_c} + \eta_3 \right) \mathrm{d}\lambda_{nc} = 0, \tag{21}$$

where the factors η_i take on the forms

$$\begin{aligned}\eta_1 &= -c_c\sqrt{n}\frac{\lambda_m}{\lambda_{nc}},\\ \eta_2 &= c_c\sqrt{n}\frac{\lambda_m^2}{\lambda_{nc}^2},\\ \eta_3 &= 2c_{nc}\alpha\left((\alpha-1)\lambda_{nc}^3(\lambda_{nc}^2-1)^{\alpha-2}+3\lambda_{nc}^2(\lambda_{nc}^2-1)^{\alpha-1}\right),\end{aligned} \tag{22}$$

and the derivative $\mathrm{d}\beta/\mathrm{d}\lambda_c$ is obtained by differentiation of the Langevin function (6), yielding

$$\frac{\mathrm{d}\beta}{\mathrm{d}\lambda_c} = \frac{1}{\sqrt{n}}\frac{1}{1-\coth^2\beta+1/\beta^2}. \tag{23}$$

Thus, by use of (22) and (23), the derivative $\mathrm{d}\lambda_{nc}/\mathrm{d}\lambda_m$ may be computed from (21), the partial derivatives in (18)–(20) may then be evaluated, which finally enables computation of the stress tensor in (17).

Once the second Piola-Kirchhoff stress tensor is established, the first Piola-Kirchhoff (nominal) stress tensor $\mathbf{P}$ and the Cauchy (true) stress tensors $\boldsymbol{\sigma}$ may be computed as

$$\mathbf{P} = \mathbf{FS}, \tag{24}$$

$$\boldsymbol{\sigma} = J^{-1}\mathbf{P}\mathbf{F}^{\mathrm{T}}. \tag{25}$$

3 Parameter Study

3.1 Prerequisites

In the present section, the influence of the five model parameters on the predicted stress-stretch relations is illustrated. We assume deformation states on the form

$$\mathbf{F} = \lambda_1\mathbf{e}_1\otimes\mathbf{e}_1+\lambda_2\mathbf{e}_2\otimes\mathbf{e}_2+\lambda_3\mathbf{e}_3\otimes\mathbf{e}_3, \tag{26}$$

where the vectors $\mathbf{e}_i$ denote basis vectors in a Cartesian coordinate system. In the following parameter study, two types of load cases are considered, i.e., uniaxial and biaxial tension. The deformation is parameterised by λ_1, and the two load cases are associated with the following deformation states:

- uniaxial tension: λ_1, $\lambda_2=\lambda_3=1/\sqrt{\lambda_1}$,
- biaxial tension: λ_1, $\lambda_2=\lambda_1$, $\lambda_3=1/(\lambda_1\lambda_2)=1/\lambda_1^2$.

By use of the boundary condition $S_{33}=0$, the Lagrange multiplier p can be explicitly expressed and determined. The principal nominal stress P_1 is computed by use of (17)–(24). Thus, for uniaxial tension, $P_1\neq 0$, $P_2=P_3=0$, and for biaxial tension, $P_1=P_2\neq 0$, $P_3=0$.

For the model parameters $c_{nc}\to\infty$, $\alpha>1$ and $c_{con}=0$, the model by Arruda and Boyce [10] is restored. As illustrated in that paper [10], the parameter choice $n=26.5$, $c_c=278$ kPa enables a good fit to the uniaxial tension data from the experiments in Treloar [41]. Thus, the model prediction for the parameter set $n=26.5$, $c_c=278$ kPa, $c_{nc}\to\infty$, and $c_{con}=0$ will be used as a reference in the following.

Two sets of experimental results from Treloar [41] will also be displayed as a reference. Treloar performed tensile testing of a vulcanized natural rubber. Testing was performed under conditions of uniaxial tension, pure shear, and biaxial tension. The experimental results for uniaxial and biaxial tension are included in the following plots.

3.2 Influence of Model Parameters

The influence of the factor c_c is trivial and is therefore left out of consideration. Thus, the role of the number of units in the representative polymer chain, n, in the model behaviour is first addressed. Figure 4 shows the model response in terms of P_1 for $n = 10$, 15, and 40. The other model parameters used are $c_c = 278$ kPa, $c_{nc} \to \infty$, $\alpha = 2$, and $c_{con} = 0$. The high stiffness assigned to c_{nc} ensures that the additional compliance from the network is negligible. It is clear from Fig. 4, that the stiffness of the material decreases with increasing value of n, provided that all other model parameters remain constant. In the absence of any additional compliance from the surrounding network, the force required to stretch a single representative polymer chain approaches infinity as $\lambda_c \to \sqrt{n}$. In Fig. 4, this is reflected by the fact that the steep rise in stress appears at lower and lower stretches as n decreases.

Next we consider the influence of the network compliance, c_{nc}. Figure 5 shows solutions for P_1, and three values of c_{nc} are investigated: 1 MPa, 10 MPa, and 100 MPa. The other

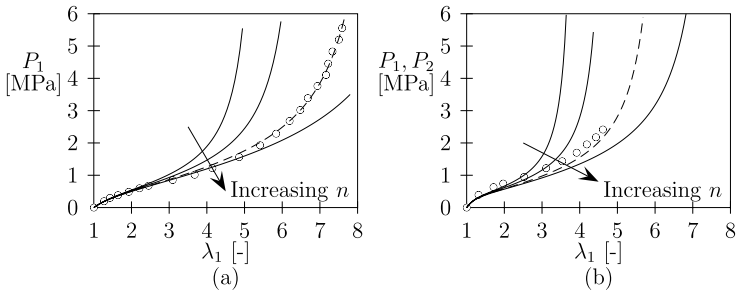

Fig. 4 Influence of model parameter n: (**a**) uniaxial tension; (**b**) biaxial tension. *Symbols* indicate experimental results from Treloar [41]. *Dashed lines* denote reference solutions from the Arruda-Boyce model [10] with $n = 26.5$ and $c_c = 278$ kPa. *Solid lines* denote solutions for the new model with $n = 10$, 15, and 40 ($c_c = 278$ kPa, $c_{nc} \to \infty$, $\alpha = 2$, and $c_{con} = 0$)

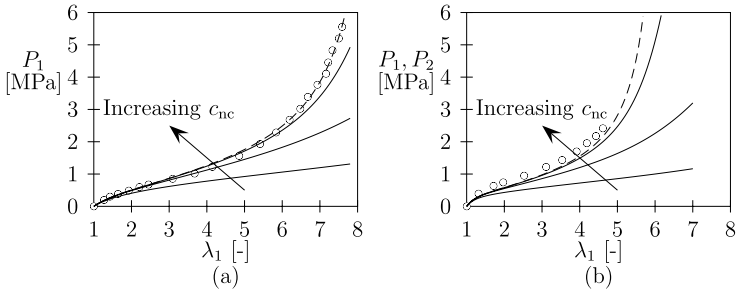

Fig. 5 Influence of model parameter c_{nc}: (**a**) uniaxial tension; (**b**) biaxial tension. *Symbols* indicate experimental results from Treloar [41]. *Dashed lines* denote reference solutions from the Arruda-Boyce model [10] with $n = 26.5$ and $c_c = 278$ kPa. *Solid lines* denote solutions for the new model with $c_{nc} = 1$ MPa, 10 MPa, and 100 MPa ($n = 26.5$, $c_c = 278$ kPa, $\alpha = 2$, and $c_{con} = 0$)

model parameters are $n = 26.5$, $c_c = 278$ kPa, $\alpha = 2$, and $c_{con} = 0$. It is clear from Fig. 5, that an increasing value of c_{nc} decreases the compliance from the network added to the representative chain, and the material therefore stiffens with increasing c_{nc}. As $c_{nc} \to \infty$, the Arruda-Boyce model is restored (provided that $c_{con} = 0$).

The network compliance has two model parameters associated with it, and we now turn to the second one, α. Figure 6 shows the predicted curves of P_1 for $\alpha = 1$, 2, and 6. The other model parameters are $n = 26.5$, $c_c = 278$ kPa, $c_{nc} = 10$ MPa, and $c_{con} = 0$. In the stretch range displayed in Fig. 6, the stress levels decrease with increasing α.

The last parameter to be considered is the stiffness c_{con}, associated with the tube constraint acting on the representative polymer chain. In Fig. 7, solutions of P_1 are shown for $c_{con} = 2$ kPa, 5 kPa, and 10 kPa (other parameters: $n = 26.5$, $c_c = 278$ kPa, $c_{nc} \to \infty$, and $\alpha = 2$). The constraint stiffness has virtually no effect at all on the model behaviour in uniaxial tension, as seen in Fig. 7(a). On the other hand, the behaviour in biaxial tension in Fig. 7(b) is significantly affected by c_{con}, and an increasing value of c_{con} tends to increase the material stiffness in biaxial tension.

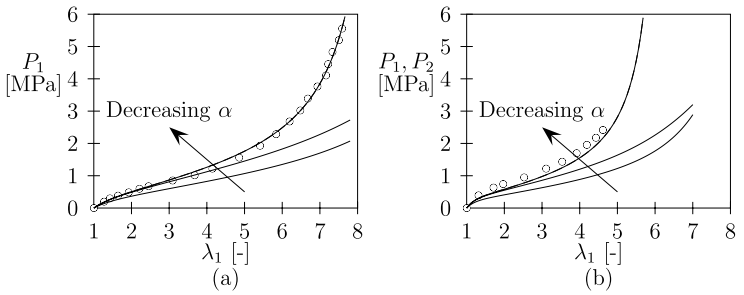

Fig. 6 Influence of model parameter α: (**a**) uniaxial tension; (**b**) biaxial tension. *Symbols* indicate experimental results from Treloar [41]. *Dashed lines* denote reference solutions from the Arruda-Boyce model [10] with $n = 26.5$ and $c_c = 278$ kPa. *Solid lines* denote solutions for the new model with $\alpha = 1$, 2, and 6 ($n = 26.5$, $c_c = 278$ kPa, $c_{nc} = 10$ MPa, and $c_{con} = 0$)

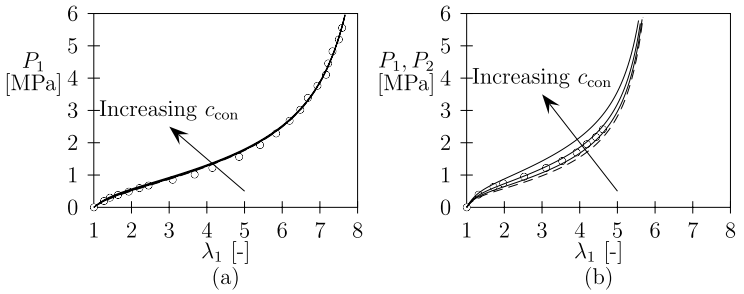

Fig. 7 Influence of model parameter c_{con}: (**a**) uniaxial tension; (**b**) biaxial tension. *Symbols* indicate experimental results from Treloar [41]. *Dashed lines* denote reference solutions from the Arruda-Boyce model [10] with $n = 26.5$ and $c_c = 278$ kPa. *Solid lines* denote solutions for the new model with $c_{con} = 2$ kPa, 5 kPa, and 10 kPa ($n = 26.5$, $c_c = 278$ kPa, $c_{nc} \to \infty$, and $\alpha = 2$)

4 Comparison with Experimental Data

4.1 Prerequisites

The purpose with the present section is to show that the proposed model correlates well with experimental data found in the literature. We again assume deformation states that may be described by principal stretches according to (26). When comparing with experimental results, three load cases are considered: (a) uniaxial tension, (b) generalised plane deformation, and (c) biaxial tension. The deformation is parameterised by λ_1, and the three load cases are associated with the following deformation states:

- uniaxial tension: λ_1, $\lambda_2 = \lambda_3 = 1/\sqrt{\lambda_1}$,
- generalised plane deformation: λ_1, $\lambda_2 = \text{constant}$, $\lambda_3 = 1/(\lambda_1\lambda_2)$,
- biaxial tension: λ_1, $\lambda_2 = \lambda_1$, $\lambda_3 = 1/(\lambda_1\lambda_2) = 1/\lambda_1^2$.

The boundary condition $S_{33} = 0$ applies in all three load cases, and the Lagrange multiplier p can again be explicitly expressed. The principal nominal stresses P_1 and P_2 are computed by use of (17)–(24). Thus, for uniaxial tension, $P_1 \neq 0$, $P_2 = P_3 = 0$, for generalised plane deformation, $P_1 \neq 0$, $P_2 \neq 0$, $P_3 = 0$, and for biaxial tension, $P_1 = P_2 \neq 0$, $P_3 = 0$.

The experimental data used to assess the model are given in terms of measurements of λ_1, λ_2, P_1, and P_2 (P_2 is not always available). The five model parameters are stored in a vector $\mathbf{q}$ according to

$$\mathbf{q} = (n \;\; c_\mathrm{c} \;\; c_\mathrm{nc} \;\; \alpha \;\; c_\mathrm{con})^\mathrm{T}. \tag{27}$$

An error function χ^2 is defined according to (cf. [42])

$$\chi^2 = \frac{1}{n_\mathrm{exp}} \left(\sum_{i=1}^{n_{\mathrm{exp},1}} \left(P_1(\lambda_1^i, \lambda_2^i, \mathbf{q}) - P_1^i \right)^2 + \sum_{i=1}^{n_{\mathrm{exp},2}} \left(P_2(\lambda_1^i, \lambda_2^i, \mathbf{q}) - P_2^i \right)^2 \right), \tag{28}$$

where λ_1^i, λ_2^i, P_1^i and P_2^i are experimental observations, $P_1(\lambda_1^i, \lambda_2^i, \mathbf{q})$ and $P_2(\lambda_1^i, \lambda_2^i, \mathbf{q})$ are the model predictions of the nominal stress components, $n_{\mathrm{exp},1}$ and $n_{\mathrm{exp},2}$ are the number of experimental observations of P_1 and P_2, respectively, and $n_\mathrm{exp} = n_{\mathrm{exp},1} + n_{\mathrm{exp},2}$ is the total number of terms included in the error function.

The error function χ^2 was minimised with respect to the model parameter vector $\mathbf{q}$ by use of the Levenberg-Marquardt algorithm [43], and in this way, an optimal set of material parameters was determined.

As a start, the model parameters were varied manually, to get an overview of where the minima appeared for the different sets of experimental data. It was concluded, that a value $\alpha = 4$ provided a good fit for all sets of data. To limit the number of unknowns in the minimisation procedure, $\alpha = 4$ was adopted throughout the analysis, and the error function was then minimised with respect to the remaining four parameters n, c_c, c_nc, and c_con.

When comparing the new constitutive model to the experimental data, the corresponding predictions by the Arruda-Boyce model [10] are also included for comparison. The curves for the Arruda-Boyce model were obtained by putting $c_\mathrm{nc} \to \infty$, $\alpha = 4$ and $c_\mathrm{con} = 0$, and then fitting n and c_c to the experimental data.

4.2 Comparison with Experimental Data from Treloar [41]

Treloar [41] performed tensile testing of a vulcanized natural rubber, and testing was performed under conditions of uniaxial tension, pure shear, and biaxial tension. Some of these

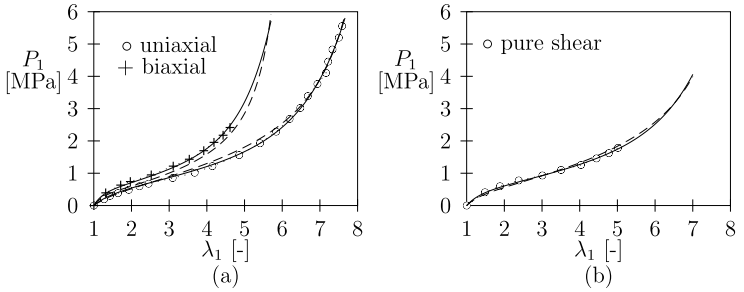

Fig. 8 The new model and the Arruda-Boyce model [10] compared with experimental data from Treloar [41] (*symbols*): (**a**) uniaxial and biaxial tension; (**b**) pure shear. *Dashed lines* denote predictions for the Arruda-Boyce model with $n = 26.9$ and $c_c = 287$ kPa. *Solid lines* denote predictions for the new model with $n = 7.38$, $c_c = 492$ kPa, $c_{nc} = 189$ kPa, $\alpha = 4$, and $c_{con} = 16.9$ kPa

data have already been shown in the parameter study in the previous section, but all sets of data from that study are now utilised. The model parameters were fitted to the experimental data, and the outcome is displayed in Fig. 8.

The predictions from the Arruda-Boyce model (dashed lines) are not too far from the experimental data, but the model is not fully able to predict the discrepancy between the cases of uniaxial and biaxial tension. Since it is the total error that is minimised (uniaxial, pure shear, and biaxial), the two predicted curves fall in between the experimental data in Fig. 8(a). On the other hand, the pure shear data in Fig. 8(b) are well predicted by the Arruda-Boyce model. This inability of the Arruda-Boyce model to predict both uniaxial and biaxial data was noted already in the original paper by Arruda and Boyce [10]. Note that since we now fit the model to all three sets of data, the estimated model parameters ($n = 26.9$ and $c_c = 287$ kPa) differ somewhat from the those obtained in that study ($n = 26.5$ and $c_c = 278$ kPa), where the model was only fitted to the uniaxial tension data.

The estimated model parameters in the new model are: $n = 7.38$, $c_c = 492$ kPa, $c_{nc} = 189$ kPa, $\alpha = 4$, and $c_{con} = 16.9$ kPa. It is clear from Fig. 8, that the new model (solid lines) is able to predict the three sets of data in a more accurate way than the Arruda-Boyce model. This pertains especially to the difference in stress levels between the cases of uniaxial and biaxial tension. The new model is able to predict the stress levels in all three load cases with a high degree of accuracy. The minimum value of the error function χ is 105 kPa and 44.6 kPa for the Arruda-Boyce and the new model, respectively, i.e. the error for the new model is about 58% lower than for the Arruda-Boyce model.

In the new model, two additions have been made to the Arruda-Boyce model (the elastic spring and the topological constraint), and it is of interest to investigate the relative importance of these two. Thus, we also made one model fitting, where $c_{con} = 0$ and parameters n, c_c, and c_{nc} were fitted to the experimental data. This yielded the estimates $n = 9.41$, $c_c = 471$ kPa, and $c_{nc} = 618$ kPa, and a final error of $\chi = 102$ kPa. In addition, we tried to put $c_{nc} \to \infty$, and then n, c_c, and c_{con} were fitted to the experiments. This yielded the estimates $n = 26.0$, $c_c = 269$ kPa, and $c_{con} = 4.44$ kPa, and the error $\chi = 58.8$ kPa. Thus, the topological constraint component of the model appears to be more important than the serial spring, but both components improve the Arruda-Boyce model in a significant way.

4.3 Comparison with Experimental Data from James et al. [44]

James et al. [44] tested a vulcanized natural rubber material. Testing was performed under conditions of generalised plane deformation, where λ_2 was kept constant. As before, we

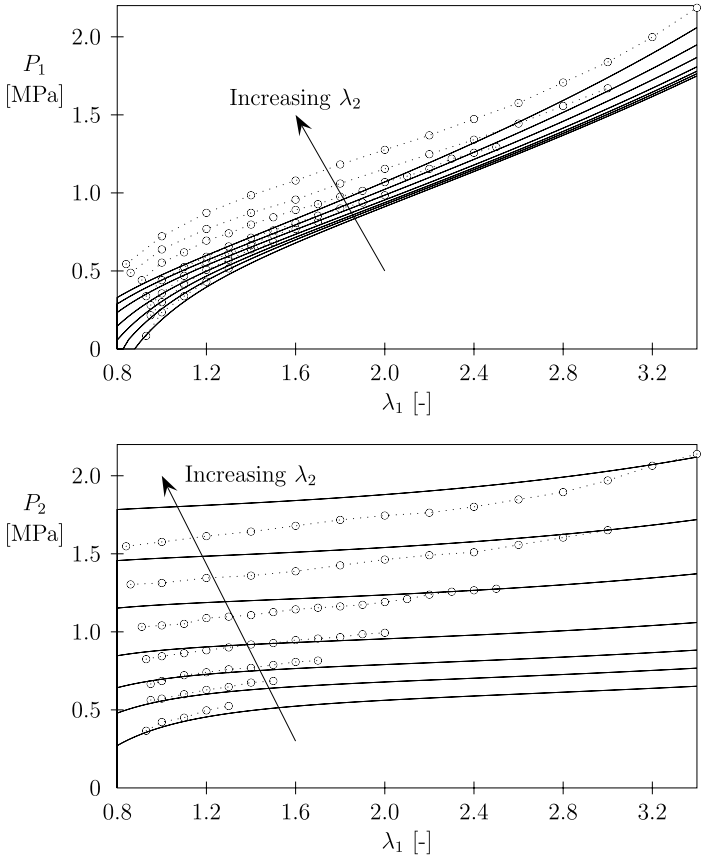

Fig. 9 Experimental data from James et al. [44] (*symbols*) and predictions for the Arruda-Boyce model [10] (*solid lines*) with $n = 21.1$ and $c_c = 446$ kPa. The different series are associated with $\lambda_2 = 1.3$, 1.5, 1.7, 2.0, 2.5, 3.0, and 3.5

start by considering the outcome when the Arruda-Boyce model is fitted to the experimental results, see Fig. 9. Results for both P_1 and P_2 are reported by James et al. [44], and the predictions of P_1 and P_2 are plotted separately for the sake of clarity. In Fig. 9, the data points connected with dotted lines indicate test series with constant λ_2. It is obvious from Fig. 9, that when the Arruda-Boyce model is fitted to these experimental data for P_1 and P_2, the mismatch between experiments and model predictions is significant. For these data, the estimated model parameters are $n = 21.1$ and $c_c = 446$ kPa. For low λ_2 stretches, the model predictions are relatively accurate, but for series with λ_2 above 2, the model becomes increasingly inaccurate for both P_1 and P_2.

The new model is also fitted to the data from James et al. [44], and the outcome is shown in Fig. 10. When minimising the error function for the new model, it was difficult to obtain a unique solution, and there appeared to be an interdependence between n and c_{nc}. In the data from James et al., the typical s-shaped character of the stress-stretch relation (as seen in Fig. 8) is not fully developed, since the maximum λ_1 stretch is 3.4. Thus, the stiffening that takes place as λ_c approaches $\sqrt{n}$ is never registered, and the fitting procedure therefore becomes underdetermined. For this reason, n was given the same value as for

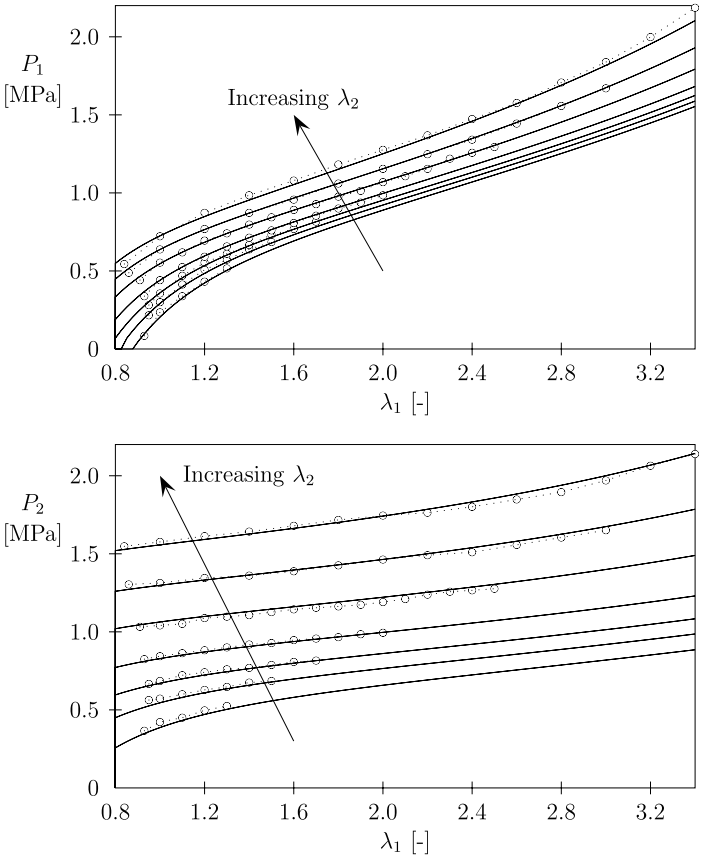

Fig. 10 Experimental data from James et al. [44] (*symbols*) and predictions for the new model (*solid lines*) with $n = 7.38$ and $c_c = 552$ kPa, $c_{nc} = 998$ kPa, $\alpha = 4$, and $c_{con} = 26.0$ kPa. The different series are associated with $\lambda_2 = 1.3$, 1.5, 1.7, 2.0, 2.5, 3.0, and 3.5

the Treloar data [41], i.e. $n = 7.38$, and the remaining parameters c_c, c_{nc}, and c_{con} were adjusted to minimise the error function. This procedure rendered the estimates $c_c = 552$ kPa, $c_{nc} = 998$ kPa, and $c_{con} = 26.0$ kPa. As can be seen from Fig. 10, the new model is able to predict the experimental data from James et al. [44] in an excellent way. The curves for series with constant λ_2 are accurately predicted both for P_1 and P_2. The minimised error functions for the Arruda-Boyce and the new model were $\chi = 104$ kPa and 18.5 kPa, respectively, implying a decrease of 82% of the error.

4.4 Comparison with Experimental Data from Kawabata et al. [45]

The third set of experiments to be used to assess the new model is from Kawabata et al. [45], who also perform tensile tests on a natural rubber vulcanizate under conditions of generalised plane deformation. Again we start by investigating to what extent the Arruda-Boyce model is able to predict the experimental outcome. For this set of experiments, the optimal set of model parameters was $n = 131$ and $c_c = 355$ kPa, and the model predictions are shown in Fig. 11. For the sake of clarity, results for P_1 and P_2 are shown separately,

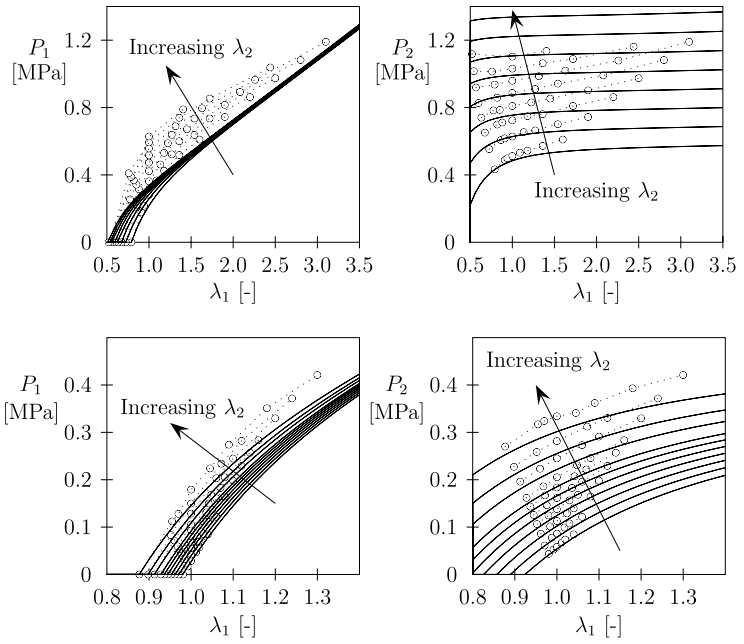

Fig. 11 Experimental data from Kawabata et al. [45] (*symbols*) and predictions for the Arruda-Boyce model [10] with $n = 131$ and $c_c = 355$ kPa (*solid lines*). *Symbols connected with dotted lines* denote series with constant λ_2. *Lower figures*: $\lambda_2 = 1.04$, 1.06, 1.08, 1.1, 1.12, 1.14, 1.16, 1.20, 1.24, and 1.30; *upper figures*: $\lambda_2 = 1.60$, 1.90, 2.20, 2.50, 2.80, 3.10, 3.40, and 3.70

and the series for different values of λ_2 are also split into two parts. The tendency is the same as before: for the test series with low λ_2, the Arruda-Boyce model is able to predict the experimental results reasonably well, but for higher values of λ_2, the predictions are clearly inaccurate.

When fitting the new model to the data from Kawabata et al. [45], we encountered the same problem as with the data from James et al. [44], i.e., there was a clear interdependence between n and c_{nc}. The reason again is that the data in Kawabata et al. [45] cover a too narrow stretch range in λ_1 to include the full *s*-shape of the material, rendering the minimisation procedure underdetermined. The value of n was therefore set to $n = 7.38$ according to the Treloar data, and the error function was then minimised with respect to the three remaining parameters. This yielded the estimates $c_c = 994$ kPa, $c_{nc} = 4.3$ kPa, and $c_{con} = 26.5$ kPa, and the associated model predictions are illustrated in Fig. 12. Again the model predictions of the new model agree extremely well with the experimental data. When comparing the Arruda-Boyce model with the new model, the error decreases from $\chi = 86.7$ kPa to 9.58 kPa, corresponding to a decrease of 89%.

5 Discussion and Concluding Remarks

Several constitutive models for rubber materials have been proposed over the last decades, but few of them have been able to accurately predict experimental results under multiaxial loading. Models based on statistical mechanics are very attractive, because they offer predictive capabilities with a minimal number of material parameters. These parameters have a

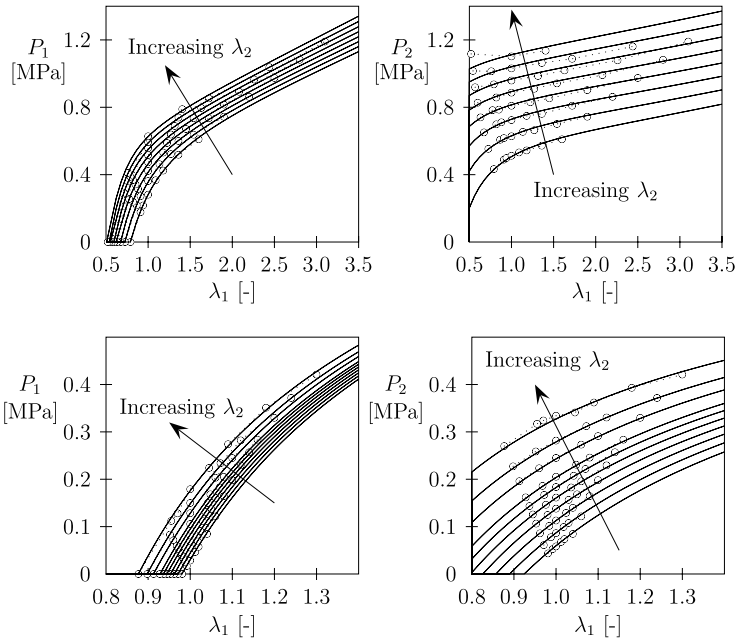

Fig. 12 Experimental data from Kawabata et al. [45] (*symbols*) and predictions for the new model with $n = 7.38$, $c_c = 994$ kPa, $c_{nc} = 4.3$ kPa, $\alpha = 4$, and $c_{con} = 26.5$ kPa. *Symbols connected with dotted lines* denote series with constant λ_2. *Lower figures*: $\lambda_2 = 1.04$, 1.06, 1.08, 1.1, 1.12, 1.14, 1.16, 1.20, 1.24, and 1.30; *upper figures*: $\lambda_2 = 1.60$, 1.90, 2.20, 2.50, 2.80, 3.10, 3.40, and 3.70

clear physical connection to the molecular microstructure, and another advantage is that the stability of these parameters is never an issue in data fitting. In the new model proposed in the present paper, we therefore start from the Arruda-Boyce model [10] and add two components to this model: an elastic spring, acting in series with the polymer chain, and a tube constraint, acting on the topology of the polymer chain. Compared with the Arruda-Boyce model, the new model includes three more model parameters, and it requires the solving of one additional non-linear equation, associated with the deformation of the serial elastic spring.

Real polymer networks do not deform affinely, and the macroscopic deformation imposed on a polymer network causes different amounts of stretching on individual polymer chains, depending on their relative length and stiffness. The introduction of a non-linear elastic spring, acting in series with the representative polymer chain and representing the additional compliance from the network surrounding, is therefore well motivated from a physical point of view. The need to account for topological constraints acting on the polymer chains is also well established, especially when multiaxial stress states are modelled. When comparing with the experimental data from Treloar [41], the model improvements (compared with the Arruda-Boyce model) were also quantified in terms of an error function. It was shown, that the introduction of the elastic spring and the topological constraint both enabled a more accurate prediction of the experimental results.

It was noted, though, that a proper determination of all five model parameters requires that tests are performed for a rather wide span in λ_1 (including the up-swing in stress at high stretches) and that multiaxial stress states are considered. Some problems were encountered

when trying to fit the new model to the data from James et al. [44] and Kawabata et al. [45], since it appeared that the minimisation procedure was underdetermined for these data.

The original Arruda-Boyce model was able to predict the constitutive behaviour of vulcanized natural rubber in uniaxial tension [10], but in equibiaxial tension, there was a significant discrepancy between model and experimental data. Arruda and Boyce actually made an attempt to improve the original model by adding the constrained network model of Flory and Erman [21, 46]. In the model by Flory and Erman, the contribution of constraints to the strain energy is somewhat more complicated than in the present model, and the contribution is given in terms of a function of the principal stretches. Through this addition, the Arruda-Boyce model behaviour was improved, but the experimental results for multiaxial loading could still not be fully modelled.

The model proposed here appears to be able to predict the constitutive behaviour in equibiaxial tension as well. In the literature, there are other models available that also are able to accurately predict the equibiaxial behaviour. One example is the model by Miehe et al. [16], which is able to predict all three sets of data (uniaxial tension, pure shear, equibiaxial tension) from Treloar [41] will a very high degree of accuracy. This model is a full network model, where non-affine chain deformations are allowed for and topological constraints on polymer chains are imposed. One significant drawback with the model proposed by Miehe et al. [16] is, however, that it requires a numerical evaluation of a surface integral. If the model is incorporated in a finite element context, this becomes very expensive from a computational point of view.

Another model that has successfully predicted the constitutive behaviour of rubber under multiaxial loading conditions is the model by Elias-Zuniga and Beatty [11]. This model is a combination of a 3-chain and an 8-chain model, and it is also able to account for all three types of data from Treloar [41]. The model by Elias-Zuniga and Beatty [11] has the advantage of only including three model parameters. It is not clear, though, to what extent this model is able to predict other cases of, say, generalised plane deformation, which has been accurately predicted by the model proposed by the present author. The model proposed here appears to have a strong ability to predict the constitutive behaviour of rubber-like solids under a wide variety of loading conditions, and it is relatively efficient from a numerical point of view. This makes it particularly suitable for implementation in a finite element context.

In summary, a new constitutive model for rubber-like solids has been proposed. The model is based on the 8-chain concept introduced by Arruda and Boyce [10], and a serial elastic spring and a topological constraint are added to the representative polymer chain characteristics. Both additions are well motivated from a physical point of view. The model contains five model parameters and these were determined on the basis of experimental data. The proposed model was able to reproduce experimental data performed under conditions of uniaxial tension, generalised plane deformation, and biaxial tension with an excellent accuracy. The strong predictive abilities together with the numerically efficient structure of the model make it suitable for implementation in a finite element context.

References

1. Guth, E., Mark, H.: Zur innermolekularen, statistik, insbesondere bei Kettenmolekülen i. Monatsh. Chem. **65**, 93–121 (1934)
2. Kuhn, W.: Über die gestalt fadenförmiger moleküle in lösungen. Kolloid-Zeitschrift **68**, 2–15 (1934)
3. Kuhn, W.: Beziehungen zwischen molekülgrösse, statistischer molekülgestalt und elastischen eigenschaften hochpolymerer stoffe. Kolloid-Zeitschrift **76**, 258–271 (1936)
4. Kuhn, W., Grün, F.: Beziehungen zwischen elastischen konstanten und dehnungsdoppelbrechung hochelastischer stoffe. Kolloid-Zeitschrift **101**, 248–271 (1942)

5. James, H.M., Guth, E.: Theory of elastic properties of rubber. J. Chem. Phys. **11**, 455–481 (1943)
6. Jernigan, R.L., Flory, P.J.: Distribution functions for chain molecules. J. Chem. Phys. **50**, 4185–4200 (1969)
7. Wang, M.C., Guth, E.: Statistical theory of networks of non-Gaussian flexible chains. J. Chem. Phys. **20**, 1144–1157 (1952)
8. Flory, P.J., Rehner, J. Jr.: Statistical mechanics of cross-linked polymer networks. J. Chem. Phys. **11**, 512–526 (1943)
9. Treloar, L.R.G.: The elasticity of a network of long-chain molecules. Trans. Faraday Soc. **42**, 83–94 (1946)
10. Arruda, E.M., Boyce, M.C.: A three-dimensional constitutive model for the large stretch behavior of rubber elastic materials. J. Mech. Phys. Solids **41**, 389–412 (1993)
11. Elias-Zuniga, A., Beatty, M.F.: Constitutive equations for amended non-Gaussian network models of rubber elasticity. Int. J. Eng. Sci. **40**, 2265–2294 (2002)
12. Treloar, L.R.G.: The photoelastic properties of short-chain molecular networks. Trans. Faraday Soc. **50**, 881–896 (1954)
13. Treloar, L.R.G., Riding, G.: A non-Gaussian theory of rubber in biaxial strain. I. Mechanical properties. Proc. R. Soc. Lond. A **369**, 261–280 (1979)
14. Wu, P.D., van der Giessen, E.: On improved network models for rubber elasticity and their applications to orientation hardening in glassy polymers. J. Mech. Phys. Solids **41**, 427–456 (1993)
15. Beatty, M.F.: An average-stretch full-network model for rubber elasticity. J. Elast. **70**, 65–86 (2003)
16. Miehe, C., Göktepe, S., Lulei, F.: A micro-macro approach to rubber-like materials—part i: the non-affine micro-sphere model of rubber elasticity. J. Mech. Phys. Solids **52**, 2617–2660 (2004)
17. Ronca, G., Allegra, G.: An approach to rubber elasticity with internal constraints. J. Chem. Phys. **63**, 4990–4997 (1975)
18. Flory, P.J.: Theory of elasticity of polymer networks. Proc. R. Soc. Lond. A **351**, 351–380 (1976)
19. Flory, P.J.: Theory of elasticity of polymer networks. The effect of local constraints on junctions. J. Chem. Phys. **66**, 5720–5729 (1977)
20. Erman, B., Flory, P.J.: Theory of elasticity of polymer networks. II. The effect of geometric constraints on junctions. J. Chem. Phys. **68**, 5363–5369 (1978)
21. Flory, P.J., Erman, B.: Theory of elasticity of polymer networks. Macromolecules **15**, 800–806 (1982)
22. Deam, R.T., Edwards, S.F.: The theory of rubber elasticity. Philos. Trans. R. Soc. A **280**, 317–353 (1976)
23. Edwards, S.F., Vilgis, R.A.: The tube model theory of rubber elasticity. Rep. Prog. Phys. **51**, 243–297 (1988)
24. Heinrich, G., Straube, E.: On the strength and deformation dependence of the tube-like topological constraints of polymer networks, melts and concentrated solutions. I. The polymer network case. Acta Polym. **34**, 589–594 (1983)
25. Heinrich, G., Straube, E.: On the strength and deformation dependence of the tube-like topological constraints of polymer networks, melts and concentrated solutions. II. Polymer melts and concentrated solutions. Acta Polym. **35**, 115–119 (1984)
26. Heinrich, G., Straube, E., Helmis, G.: Rubber elasticity of polymer networks: theories. Adv. Polym. Sci. **85**, 33–87 (1988)
27. Horgan, C.O., Saccomandi, G.: Phenomenological hyperelastic strain-stiffening constitutive models for rubber. Rubber Chem. Technol. **79**, 152–169 (2006)
28. Mooney, M.: A theory of large elastic deformation. J. Appl. Phys. **11**, 582–592 (1940)
29. Rivlin, R.S.: Large elastic deformations of isotropic materials IV. Further developments of the general theory. Philos. Trans. R. Soc. A **241**, 379–397 (1948)
30. Gent, A.N.: A new constitutive relation for rubber. Rubber Chem. Technol. **69**, 59–61 (1996)
31. Gent, A.N.: Extensibility of rubber under different types of deformation. J. Rheol. **49**, 271–275 (2005)
32. Yeoh, O.H.: Some forms of the strain energy function for rubber. Rubber Chem. Technol. **66**, 754–771 (1993)
33. Beda, T.: Modeling hyperelastic behavior of rubber: A novel invariant-based and a review of constitutive models. J. Polym. Sci., Polym. Phys. **45**, 1713–1732 (2007)
34. Valanis, K.C., Landel, R.F.: The strain-energy function of a hyperelastic material in terms of the extension ratios. J. Appl. Phys. **38**, 2997–3002 (1967)
35. Ogden, R.W.: Large deformation isotropic elasticity—on the correlation of theory and experiment for incompressible rubberlike solids. Proc. R. Soc. Lond. A **326**, 565–584 (1972)
36. Fried, E.: An elementary molecular-statistical basis for the Mooney and Rivlin-Saunders theories of rubber elasticity. J. Mech. Phys. Solids **50**, 571–582 (2002)
37. Doi, M., Edwards, S.F.: The Theory of Polymer Dynamics, 1st edn. Clarendon Press, Oxford (1986)
38. Horgan, C.O., Saccomandi, G.: Simple torsion of isotropic, hyperelastic, incompressible materials with limiting chain extensibility. J. Elast. **56**, 159–170 (1999)

39. Pucci, E., Saccomandi, G.: A note on the Gent model for rubber-like materials. Rubber Chem. Technol. **75**, 839–852 (2002)
40. Wineman, A.: Some results for generalized neo-Hookean elastic materials. Int. J. Non-Linear Mech. **40**, 271–279 (2005)
41. Treloar, L.R.G.: Stress-strain data for vulcanized rubber under various types of deformation. Trans. Faraday Soc. **40**, 59–70 (1944)
42. Ogden, R.W., Saccomandi, G., Sgura, I.: Fitting hyperelastic models to experimental data. Comput. Mech. **34**, 484–502 (2004)
43. Press, W., Teukolsky, S., Vetterling, W., Flannery, B.: Numerical Recipes in C. The Art of Scientific Computing, 2nd edn. Cambridge University Press, Cambridge (1994)
44. James, A.G., Green, A., Simpson, G.M.: Strain energy functions of rubber. I. Characterization of gum vulcanizates. J. Appl. Polym. Sci. **19**, 2033–2058 (1975)
45. Kawabata, S., Matsuda, M., Tei, K., Kawai, H.: Experimental survey of the strain energy density function of isoprene rubber vulcanizate. Macromolecules **14**, 154–162 (1981)
46. Boyce, M.C., Arruda, E.M.: Constitutive models of rubber elasticity: a review. Rubber Chem. Technol. **73**, 504–523 (2000)